

## **EFFICIENT EVALUATION OF GREEN'S FUNCTIONS FOR LOSSY HALF-SPACE PROBLEMS**

**Z. H. Firouzeh and G. A. E. Vandenbosch**

ESAT-TELEMIC

Kasteelpark Arenberg 10 bus 2444, B-3001 Leuven, Belgium

**R. Moini and S. H. H. Sadeghi**

Electrical Engineering Department  
Amirkabir University of Technology  
424 Hafez Avenue, Tehran 15914, Iran

**R. Faraji-Dana**

School of Electrical and Computer Engineering  
University of Tehran  
Kargar Ave. North, P. O. Box 14395-515, Tehran, Iran

**Abstract**—In this paper, a new technique is developed to evaluate efficiently the Sommerfeld integrals arising from the problem of a current element radiating over a lossy half-space. The annihilation of the asymptote and the branch-point singular behavior of the spectral Green's function is used in this technique. The contributions of the subtracted asymptotic and singularity terms are calculated analytically. The annihilation results in a remaining integral that is very smooth and can be calculated adaptively by using Gaussian quadratures and extrapolation methods to accelerate the convergence of the oscillating integrand. The accuracy and efficiency of the new technique has been confirmed by comparison with literature, and the commercial software NEC. The application of the proposed technique provides a robust and rapid procedure to calculate spatial Green's functions which can be used in ground-wave propagation, and lightning return stroke channel modeling.

## 1. INTRODUCTION

The numerical analysis of electromagnetic wave interaction in half-space problems is important for a variety of applications such as linear antennas near earth or ocean surface, ground-wave propagation, geophysical prospecting, grounding systems, and lightning return stroke channel modeling [1–5]. The radiation characteristics of a dipole source above a dissipative half-space was first introduced by Sommerfeld in 1909 [6]. The solution was given in terms of integrals, presently called Sommerfeld integrals (SIs). Later, he discussed and extended this problem much more in [7]. Then, a comprehensive formulation on the development of the lossy half-space problem, using Hertz potentials, was given by Banos [8].

There have been published many numerical and analytical techniques to deal with the integrals arising in the Sommerfeld half-space problem, which have been reviewed in [9–12]. A fundamental fact is that the occurring Sommerfeld integrals cannot be evaluated in closed form. The analytic methods described are based on approximations, which can be used for only a limited range of parameters. Numerical techniques have difficulties in accurately evaluating the Sommerfeld integrals. This is due to the highly oscillatory and slowly converging behaviour of the integrand, and to its singularities, including branch points and a virtual pole near the real-axis path of integration in the  $k_\rho$ -plane [11].

A direct numerical integration of SI is generally useful in near-field regions [13–19]. The numerical integration on the real-axis path (path A in Fig. 1) was first done by Siegel and King [13]. Direct integration

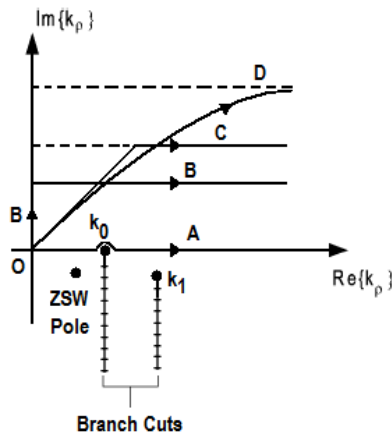


**Figure 1.** Different integration paths in the complex  $k_\rho$ -plane [12].

using Simpson's rule or other quadratures was also applied by Tsang et al. [14]. They used fast Fourier transform (FFT) to expand a part of the integrand which has known integrals to reduce the computation time. The real-axis path has been used in related problems by Kuo and Mei [15], Lin and Mei [16], Katehi and Alexopoulos [17], Johnson and Dudley [18], and Michalski [19]. Highly accurate numerical integration techniques can be used for any set of parameters of the lossy ground. However, these procedures suffer from high computational complexity.

Other authors prefer to deform the original path of integration to a contour off the real axis, based on Cauchy's theorem for analytic functions, to avoid the difficulties associated with the presence of singularities. If transformations of the integration path are performed, the convergence is improved, but the formulation becomes more complicated. For example, path B (Fig. 1) is used by Miller et al. [20] and Sarkar [21], but Burke et al. [10] have employed path C. Integration along the vertical branch cuts as shown in Fig. 1 [22, 23], and more complicated integration paths have also been used [24].

There are various asymptotic solutions for different ranges of relative source-observation distance. An asymptotic far-field evaluation was done by Yokoyama [25], while Chang and Wait [26] developed the near-field approximation. Kuo [27] assumed a large refractive index to transform the SI to fast-convergent forms with the aid of several approximations. Expressions for several forms of SI in terms of incomplete Hankel functions were given by Chang and Fisher [28]. Another approach is to expand part of the integrand in a special form which has known integrals. Lindsay [29] used spline functions to represent part of the integrand and the resulting integrals were then evaluated in terms of Lommel functions. The image-theory approximation was developed by Wait [30], who represented the reflection function in terms of exponentials in the integrals. This approximation is valid for a low frequency or a large dielectric permittivity. The image-theory extension to an arbitrary quasi-static source was done by Weaver [31]. The image-theory accuracy was demonstrated by Bannister [32] through comparison with available analytical and numerical results. The effect of the earth's permeability and displacement currents were neglected in these formulations. One efficient method has been to approximate the Fourier transform of the field by an expression that can be transformed back to the physical space introduced by Mittra et al. [33]. Also, composite multipole images for different kind of sources by using the FFT [14] are employed by Mohsen [11]. Using these two techniques results in a small computation time and a wide range of applicability. However, it has not been easy to see the range of validity for the different image systems.

Using a unified analytical approach, four image representations for sources of vertically polarized waves above a conducting surface have been introduced by Mahmoud [34]. This approach is computationally simple, but only a limited range of parameters can be considered. Lindell et al. [35–38] used the continuous image theory for an electric or a magnetic dipole in a half space to calculate the reflected fields in the same half-space [35–37] or the transmitted fields in the other half-space [38]. Xu and Huang [39] analyzed efficiently a vertical thin-wire antenna above a lossy halfspace by reducing the Sommerfeld-type integrals to semi-infinite integrals that converge rapidly using the exact image theory.

Another important integration method is the steepest descent path (SDP) method. Direct numerical integration consumes a large amount of computer time in far-field regions. However the saddle-point technique is used along the SDP instead of the Sommerfeld integration path (SIP) [40–42] for the asymptotic approximation of the integrals [43, 44]. This path of integration is superior to other approaches in far-field regions since this method in the limit leads to the geometrical optics technique, which is known to have a low calculation time consumption. In this method, the contributions of proper surface and leaky wave modes should be included, and hence a technique for locating the modes should be considered. For this, techniques have been developed based on several approximate analytical expressions for a wide variety of conditions. The range of applicability of these expressions depends upon the frequency and the relative locations of source point, observation point, and ground, as well as the medium parameters such as permittivity, permeability, and conductivity. Rahmat-Samii et al. [9] have found, however, that the integration along the SDP is very efficient even for distances less than in the far-field region. The combination of asymptotic and exact evaluation of these integrals can efficiently compute the spatial Green's functions [45], but the computational complexity is high. However, there are a few difficulties with the SDP method. One difficulty is due to the virtual pole of the integrand, i.e., the Zenneck surface-wave (ZSW) pole [43, 46], which can be close to the SDP when both the source and the observation points are close to the interface and the contrast between the two media is large. In that case, the integrand behavior on the SDP exhibits a sharp variation close to the Zenneck surface-wave pole, requiring a very careful integration. Tsang and Kong [47] coped with that by calculating the saddle point contribution in near-field regions by using the Gaussian hermite quadrature formula. Furthermore, in intermediate regions and in far-field zones, the modified saddle point method (MSP) should be used

when there are poles near the saddle point. Another issue is the fact that the position of the SDP should be monitored constantly with respect to the branch cuts in order to use the most efficient contour of integration [48]. Michalski and Butler introduced an efficient analytic expression on a new SDP, which is qualitatively represented as contour D in Fig. 1, when the source and field points are in different media [12]. This path avoids the real-axis singularities and is the SDP for the exponential function part of the integrand, leading to a fast and accurate calculation in far-field regions. Recently, the numerically modified steepest descent path method (NMSP) has been used for thin layers [49]. The NMSP method is an extension of the MSP [47], which consists of the extraction of the poles and the numerical evaluation of the SDP by using a much lower quadrature. Therefore, the contribution due to these pole and branch point singularities must be taken into account in the SDP method, leading to a high complexity and time-consumption.

In general, several approaches have been developed for the numerical evaluation of Sommerfeld integrals occurring in the calculation of multi-layered media spatial Green's functions. The traditional method is the integration over the real axis combined with pole extraction techniques and averaging methods, leading to a very efficient algorithm [50]. This technique is very efficient for relatively small source-observer distances. For large source-observer distances it is usually required to integrate functions exhibiting abrupt variations and fast oscillating behaviors. To overcome this problem, several extrapolation methods have been introduced to accelerate convergence of Sommerfeld-type integral tails, which explicitly utilize remainder estimates. This proves to be particularly effective and accurate. Michalski [51] has presented a review of the most promising extrapolation methods for the acceleration of Sommerfeld-type integral tails to give rapid and accurate results. Mosig et al. presented another efficient technique for the numerical evaluation of Sommerfeld integrals [52, 53]. They choose a new integration contour that is closed by the imaginary axis of the spectral plane. This results in improper integrals involving fast decaying modified Bessel functions  $K_n$  along the imaginary axis, which results in very fast converging integrals, and thus less computational effort. Demuynck et al. [54] developed an accurate and computationally efficient procedure to calculate spatial Green's functions using asymptotic and singularity subtraction methods. First, the asymptotic behavior of the spectral-domain Green's function at high spectral values is removed. Its inverse is added analytically in the spatial domain. In addition, the spectral Green's function shows singular behavior due to the existence of poles and branch points

located along the real axis. This behavior, both due to poles and branch points, can also be subtracted in the spectral domain, and re-added analytically in the spatial domain. The singular behavior due to the branch points can be associated with the existence of half-spaces in the layer structure. The remaining spectral function along the real axis is a smooth and fast decaying function, which can be integrated numerically. It is important to note that the technique of [54] cannot be applied directly to multi-layered media with two open-half spaces. Simsek et al. [55] presented a procedure to subtract analytically singularity terms causing a slow convergence. This procedure can be described as an improved version of the extraction procedure implemented in the discrete complex image method (DCIM) [56]. Each individual term of the integrand and the contribution of the subtracted terms is calculated analytically. The remaining integral is calculated numerically by using Gaussian quadratures.

In the present study, we propose improvements to [54] to be able to use it for double half-space problems. So, basically, asymptotic and branch-point singularity subtraction functions with analytical spatial equivalents are used. This leads to a remaining spectral function along the real axis which is very smooth and fast decaying, and can be integrated numerically. For near and intermediate regions, this can be done by using Gaussian quadratures. For far regions, it is necessary to use extrapolation methods to accelerate the convergence of the Sommerfeld-type integral tail [51]. The rest of the paper is organized as follows. The algorithm of the proposed numerical method is described in Section 2. The validity of the proposed method is examined in Section 3, where it is compared with commercial software such as the Numerical Electromagnetic Code (NEC) and [50]. Concluding remarks are given in Section 4.

## 2. EFFICIENT CALCULATION OF THE HALF-SPACE GREEN'S FUNCTIONS

Consider a lossy medium in the half space  $z < 0$  characterized by the relative dielectric constant  $\epsilon_r$ , conductivity  $\sigma$ , and wave number

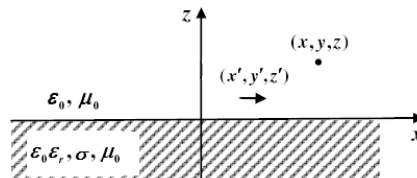


**Figure 2.** An electrical dipole above a lossy ground.

$k_1$ . The upper half space  $z > 0$  is vacuum, with permittivity  $\epsilon_0$ , permeability  $\mu_0$ , and wave number  $k_0$ . A horizontal electric dipole (HED) of unit strength is located at height  $z'$  above the medium, as shown in Fig. 2. The proposed method can be applied to all the spectral-domain Green's functions of the HED, but here it is explained only for the spectral-domain scalar potential  $\tilde{G}_q$  in the air region.  $\tilde{G}_q$  can be represented as follows [56, 57]:

$$\tilde{G}_q = \frac{1}{4\pi\epsilon_0} \frac{1}{2jk_{z0}} \left[ e^{-jk_{z0}|z-z'|} + (R_{TE} + R_q) e^{-jk_{z0}(z+z')} \right] \quad (1)$$

$$R_{TE} = \frac{k_{z0} - k_{z1}}{k_{z0} + k_{z1}} \quad (2)$$

$$R_q = \frac{2k_{z0}^2(1 - \epsilon'_r)}{(k_{z0} + k_{z1})(\epsilon'_r k_{z0} + k_{z1})} \quad (3)$$

$$k_{z0}^2 + k_\rho^2 = k_0^2, \text{Im}\{k_{z0}\} \leq 0 \quad k_{z1}^2 + k_\rho^2 = k_1^2, \text{Im}\{k_{z1}\} \leq 0 \quad (4)$$

$$k_0^2 = \omega^2 \mu_0 \epsilon_0 \quad k_1^2 = \omega^2 \mu_0 \epsilon'_r \epsilon_0 \quad \epsilon'_r = \epsilon_r - j\sigma/\omega\epsilon_0 \quad (5)$$

$k_\rho$  is the radial wave number and  $k_{zi}$  is the wave number in the  $z$ -direction in medium  $i$  ( $i = 0$  for vacuum and  $i = 1$  for the dielectric). The time variation  $e^{j\omega t}$  is assumed throughout this paper and suppressed.

The spatial-domain  $G_q$  is the inverse Fourier transform of its spectral equivalent. It can be calculated as a Sommerfeld integral given by [52]

$$G_q = \int_{-\infty}^{\infty} H_0^{(2)}(k_\rho \rho) k_\rho \tilde{G}_q(k_\rho) dk_\rho \quad (6)$$

where  $H_0^{(2)}$  is the Hankel function of the second kind and order zero.  $\rho$  is the horizontal distance between the source and observation point. The asymptotic behavior of  $k_\rho \tilde{G}_q(k_\rho)$  for large  $k_\rho$  determines the contribution in the neighborhood of the source because the oscillation period of the Hankel function is very large for low  $\rho$ . The decay of  $k_\rho \tilde{G}_q(k_\rho)$  is very slow. Therefore, the so-called direct and reflected terms are easily subtracted from (1) to improve the convergence of the integration. The contribution of these components to (6) can be calculated analytically by using the Sommerfeld identity [56]. After some mathematical manipulation, we obtain

$$G_q = \frac{1}{4\pi\epsilon_0} \left( \frac{e^{-jk_0 r_0}}{r_0} + \frac{1 - \epsilon'_r}{1 + \epsilon'_r} \frac{e^{-jk_0 r'_0}}{r'_0} \right) + I_1 \quad (7)$$

$$I_1 = \frac{1}{\pi\varepsilon_0(1+\varepsilon'_r)} \int_0^\infty \frac{1}{2jk_{z0}} \left( \frac{k_{z0}-k_{z1}}{\varepsilon'_r k_{z0}+k_{z1}} \right) e^{-jk_{z0}(z+z')} J_0(k_\rho \rho) k_\rho dk_\rho \quad (8)$$

$$r_0 = \sqrt{\rho^2 + (z - z')^2}, \quad r'_0 = \sqrt{\rho^2 + (z + z')^2} \quad (9)$$

where  $J_0$  is the Bessel function of the first kind and order zero. The singular behavior of  $k_\rho \tilde{G}_q(k_\rho)$  governs the result spatially further away from the source. There are no proper poles for a half-space medium in the upper Riemann sheet to be taken into account. However, when Cauchy's residue theorem is used to convert the integral on the real axis in the  $k_\rho$ -plane into a contour integral over the entire complex  $k_\rho$ -plane, a Zenneck surface wave pole should be taken into account. Particularly, when the ground has a large dissipation, and source and observation points are near to or on the interface, the virtual pole is very close to the saddle point [43]. In that case, the integrand behavior on the SDP exhibits a sharp variation close to the Zenneck surface wave pole, requiring a very careful integration, for example with the MSP method [47]. However, the improper poles responsible for the Zenneck surface waves are hardly excited by a highly localized source [2]. In the available references [58–61], more details about the excitation and characteristics of the surface waves in a multi-layered region are found.

Since the problem consists of two semi-infinite regions, there are two branch point singularities corresponding to the wave numbers of each region. They are responsible for the far-field behavior of the field components. The branch points represent the continuous spectrum and appear as lateral waves in the far field [2, 53]. Also, one needs to consider the effect of the branch point related to the free space wave number only, since the contribution of the other branch point is inferior due to the lossiness of the medium. Therefore, the only type of singularity that occurs in the numerical integration of (8) is at the branch point  $k_\rho = k_0$ . A new function is proposed to annihilate this singularity. It shows the following characteristics: 1) the behavior of the function in the neighborhood of the singularity is the same as the behavior of the Green's function; 2) the inverse Fourier transform of the function is known analytically in closed form; and 3) the asymptotic behavior for large  $k_\rho$  of the function decays faster than the asymptote of the original Green's function in order not to influence the subtraction procedure of the direct term. The new function is

$$\tilde{f}(k_\rho) = -\frac{1}{2jk_{z0}} + \frac{1}{2\sqrt{k_\rho^2 + k_0^2}} \quad (10)$$

The first part of  $\tilde{f}(k_\rho)$  is used to annihilate the singular behavior at  $k_\rho = k_0$ . The second one is necessary for large  $k_\rho$  in order to make

the decay there large enough to avoid the introduction of a spatial singularity at the origin. The analytical functions calculated by the inverse Fourier transform are [62]

$$f(\rho) = -\frac{e^{-jk_0\rho}}{\rho} + \frac{e^{-k_0\rho}}{\rho} \quad (11)$$

After the removal of the asymptote and the branch-point singularity from the spectral Green's function,  $G_q$  can be calculated as

$$G_q = \frac{1}{4\pi\epsilon_0} \left[ \frac{e^{-jk_0r_0}}{r_0} + \frac{1-\epsilon'_r}{1+\epsilon'_r} \frac{e^{-jk_0r'_0}}{r'_0} + \frac{2}{1+\epsilon'_r} \left( -\frac{e^{-jk_0\rho}}{\rho} + \frac{e^{-k_0\rho}}{\rho} \right) \right] + I_2 \quad (12)$$

$$I_2 = \frac{1}{\pi\epsilon_0(1+\epsilon'_r)} \int_0^\infty \left( \frac{1}{2jk_{z0}} \frac{k_{z0}-k_{z1}}{\epsilon'_r k_{z0} + k_{z1}} e^{-jk_{z0}(z+z')} - \tilde{f}(k_\rho) \right) J_0(k_\rho \rho) k_\rho dk_\rho \quad (13)$$

In a similar manner and with a few simple mathematical manipulations, the x component of the magnetic vector potential  $G_{xx}^A$  can be calculated as follows.

$$G_{xx}^A = \frac{\mu_0}{4\pi} \left( \frac{e^{-jk_0r_0}}{r_0} - \frac{e^{-jk_0\rho}}{\rho} + \frac{e^{-k_0\rho}}{\rho} \right) + \frac{\mu_0}{2\pi} \int_0^\infty \left( \frac{1}{2jk_{z0}} R_{TE} e^{-jk_{z0}(z+z')} - \tilde{f}(k_\rho) \right) J_0(k_\rho \rho) k_\rho dk_\rho \quad (14)$$

For a vertical electric dipole (VED) of unit strength, the spatial-domain Green's function for the z component of the electric field  $G_z^{EJ}$  in the upper region is given by [63]

$$G_z^{EJ} = -j\omega G_{zz}^A + \Phi_z^d \quad (15)$$

$$G_{zz}^A = \frac{\mu_0}{4\pi} \left( \frac{e^{-jk_0r_0}}{r_0} - \frac{1-\epsilon'_r}{1+\epsilon'_r} \frac{e^{-jk_0r'_0}}{r'_0} \right) + \frac{\mu_0}{4\pi} \left( \frac{2\epsilon'_r}{1+\epsilon'_r} \right) I_3 \quad (16)$$

$$I_3 = 2 \int_0^\infty \frac{1}{2jk_{z0}} \left( \frac{k_{z0}-k_{z1}}{\epsilon'_r k_{z0} + k_{z1}} \right) e^{-jk_{z0}(z+z')} J_0(k_\rho \rho) k_\rho dk_\rho \quad (17)$$

$$\Phi_z^d = \frac{-1}{j4\pi\omega\epsilon_0} \frac{\partial^2}{\partial z \partial z'} \left( \frac{e^{-jk_0r_0}}{r_0} + \frac{1-\epsilon'_r}{1+\epsilon'_r} \frac{e^{-jk_0r'_0}}{r'_0} \right) + \frac{1}{j4\pi\omega\epsilon_0} \left( \frac{2\epsilon'_r}{1+\epsilon'_r} \right) I_4 \quad (18)$$

$$I_4 = \int_0^\infty jk_{z0} \left( \frac{k_{z0}-k_{z1}}{\epsilon'_r k_{z0} + k_{z1}} \right) e^{-jk_{z0}(z+z')} J_0(k_\rho \rho) k_\rho dk_\rho \quad (19)$$

The integral  $I_3$  has the branch-point singularity at  $k_\rho = k_0$ . After the removal of the asymptote and the branch-point singularity from the spectral Green's function,  $I_3$  can be calculated as

$$I_3 = -\frac{e^{-jk_0\rho}}{\rho} + \frac{e^{-k_0\rho}}{\rho} + 2 \int_0^\infty \frac{1}{2jk_{z0}} \left( \frac{k_{z0} - k_{z1}}{\varepsilon_r' k_{z0} + k_{z1}} e^{-jk_{z0}(z+z')} - \tilde{f}(k_\rho) \right) J_0(k_\rho\rho) k_\rho dk_\rho \quad (20)$$

Finally, the remaining spectral functions in (13), (14), and (20) along the real axis are smooth and fast decaying functions, which can be integrated numerically. For near and intermediate regions, the integrals in (13), (14) and (20) can be computed by using Gaussian Laguerre interpolatory quadratures [21]. For far regions, especially when the source and field points are on the interface, the  $W$  transformation and the weighted-averages method (WAM) emerge as the most efficient extrapolation methods to accelerate the convergence of the Sommerfeld-type integral tails [51].

### 3. NUMERICAL RESULTS

The accuracy and efficiency of the proposed method is verified by considering numerical examples. The first example is a lossy half-space medium with  $\varepsilon_r = 10$  and  $\sigma = 0.1$  S/m, as shown in Fig. 2, analyzed at 1 GHz. Both the source and observation points are on the interface, i.e., at  $z = z' = 0$ . The behavior of the integrand of  $I_1$  in (8) (before the subtraction) and that of  $I_2$  in (13) (after the subtraction) are depicted for different  $\rho$ 's. Fig. 3 shows a typical example of the type of function to be integrated, in this case for  $k_0\rho = 10$ . An enlarged view in the interval  $[0.99k_0, 1.01k_0]$  is depicted in the same figure. The numerical integration is challenging because of the strong variations close to the branch-point singularity, a consequence of the infinite derivative at  $k_\rho = k_0$ . After subtraction of the branch-point singularity, i.e.,  $\tilde{f}(k_\rho)$ , from the integrand, the infinite derivative in  $k_0$  is eliminated. The resulting function is much smoother, as shown in Fig. 4. Fig. 5 shows the effect of the subtractions in a higher interval. The resulting function is a smooth and fast decaying function that can easily be integrated by using Gaussian Laguerre interpolatory quadratures in the near and intermediate region. In the far region however, it can be adaptively integrated in the interval  $[0, k_0\sqrt{\varepsilon_r}]$  by using Gaussian quadratures, and in the region  $[k_0\sqrt{\varepsilon_r}, \infty]$  by using the weighted-averages method (WAM).

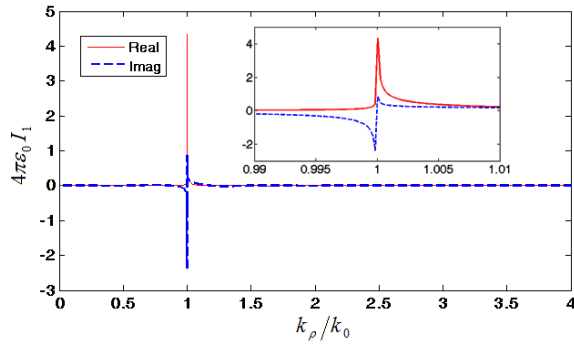


**Figure 3.** Real and imaginary parts of the integrand  $4\pi\epsilon_0 I_1$  before the subtraction of the branch-point at  $k_\rho = k_0$ .

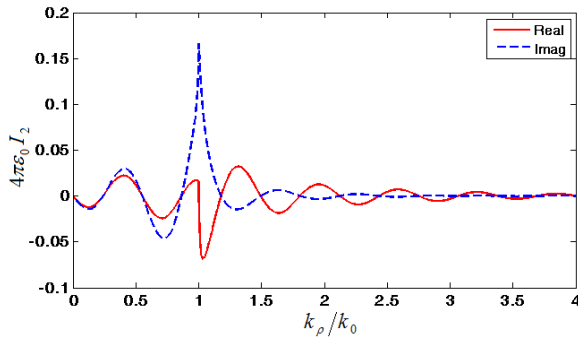


**Figure 4.** Real and imaginary parts of the integrand  $4\pi\epsilon_0 I_2$  after the subtraction of the branch-point at  $k_\rho = k_0$ .

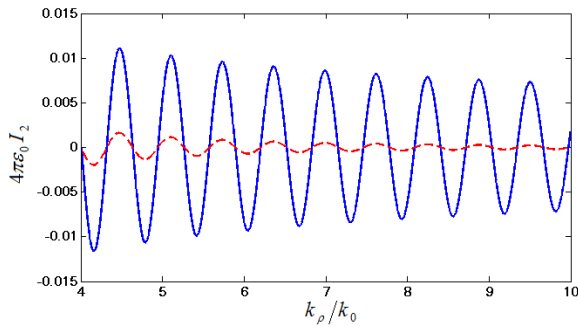


**Figure 5.** Real part of the integrands in the interval  $[4k_0, 10k_0]$  before (the solid line) and after (the dashed line) the subtraction of the asymptotic and branch point contributions.

The amplitudes of  $G_q$  and  $G_{xx}^A$  are depicted in Figs. 6 and 7, respectively, in the range  $10^{-3} \leq k_0\rho \leq 10^4$  for three frequencies: 10 MHz, 100 MHz, and 1 GHz. The numerical results obtained by the proposed method are compared with those obtained using Mosig's method [50]. The agreement is almost perfect. In addition, the first part of (12) and (14) is also shown in the near field zone, where the field is dominated by the quasi-static term, showing a  $1/\rho$  behavior. The continuous spectrum results in the overall  $(1/\rho^2)$  dependence for large source-observer distances [53]. Table 1 compares the computation times of the proposed method and Mosig's method [50] to calculate  $G_q$  in the range  $10^{-3} \leq k_0\rho \leq 10^4$  (700 points). The computer used in this comparison has an Intel Core 2 CPU 2.13 GHz processor and 2 GB of RAM. The new technique is considerably faster.

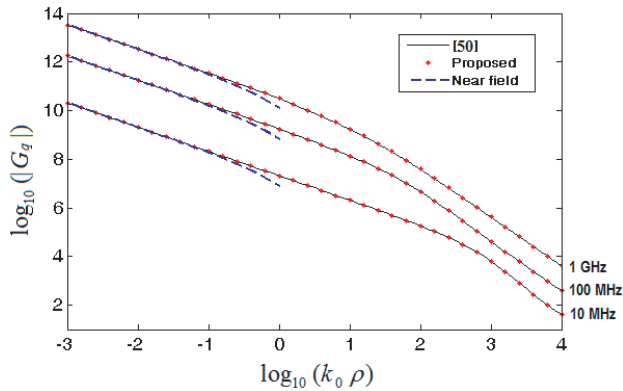


**Figure 6.** The amplitude of  $G_q$  at 10 MHz, 100 MHz, and 1 GHz.

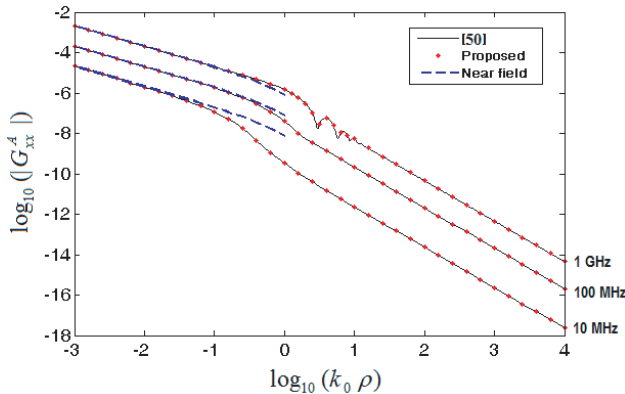


**Figure 7.** The amplitude of  $G_{xx}^A$  at 10 MHz, 100 MHz, and 1 GHz.

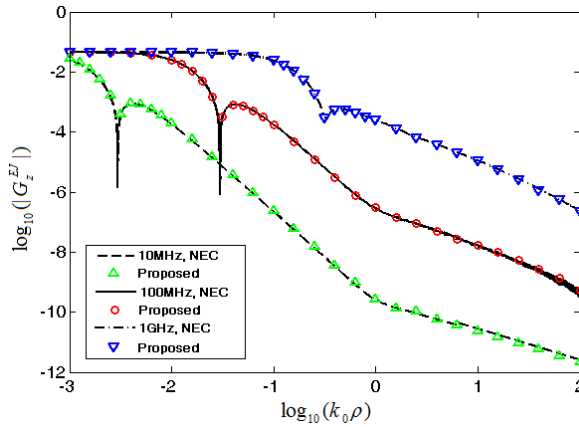


**Figure 8.** The amplitude of  $G_z^{EJ}$  at 10 MHz, 100 MHz, and 1 GHz.

**Table 1.** Comparison of the computation times to calculate  $G_q$ .

Frequency	Proposed method	Method of [50]
10 MHz	127.136 sec	416.192 sec
100 MHz	139.310 sec	486.505 sec
1000 MHz	150.925 sec	588.514 sec

The second example is more complex. It involves losses and the proper combination of vector and scalar potential Green’s functions in order to obtain directly the Green’s function for an electric field component. Consider a vertical electric dipole (VED) located at  $z' = 10$  mm above the previous lossy ground. The spatial Green’s function for the  $z$  component of the electric field vector  $G_z^{EJ}$  in the upper region on the interface, i.e., at  $z = 0$ , is computed with the proposed technique. The results are compared to the Numerical Electromagnetic Code (NEC) in Fig. 8, in the range  $10^{-3} \leq k_0\rho \leq 10^2$  for different frequencies (10 MHz, 100 MHz, and 1 GHz). Again, the agreement is almost perfect for all field regions. The proposed technique is very simple and efficient compared to NEC, in which the Sommerfeld integrals are evaluated by numerical integration along contour C in Fig. 1, using lookup tables, interpolation methods, and higher-order asymptotic approximations, in order to cover the entire distance [64].

#### 4. CONCLUSION

In this paper, a new, simple and efficient technique for the evaluation of Sommerfeld integrals occurring in lossy half-space problems is described. In this technique, the asymptotic and branch-point singularity behaviors of the spectral Green's functions, yielding a slow convergence, have been subtracted. Their contribution is added again analytically in the spatial domain. No matter how close the source and field points are to the interface or no matter how large the distance between source and observation point is, the described annihilation procedure returns a remaining integrand that is smooth and fast decaying along the real axis. Consequently, it can be computed by using a variety of methods well-known in literature. The accuracy, efficiency, and speed of the technique have been verified via representative numerical examples. The main advantages of the proposed technique are its generality, relative simplicity, the capability to implement it in a straightforward way in the case of multilayered structures, and the very low computation time compared to other techniques. It can be used in a variety of applications, such as ground-wave propagation, geophysical prospecting, and lightning return stroke channel modeling.

#### ACKNOWLEDGMENT

This work has been supported by the Iran Telecommunication Research Center (ITRC).

#### REFERENCES

1. Arand, B. A., M. Hakkak, K. Forooraghi, and J. R. Mohassel, "Analysis of aperture antennas above lossy half-space," *Progress In Electromagnetics Research*, Vol. 44, 39–55, 2004.
2. Wait, J. R., "The ancient and modern history of EM ground-wave propagation," *IEEE Antenna & Propag. Magazine*, Vol. 40, No. 5, 7–24, Oct. 1998.
3. Daniels, D. J., *Ground Penetrating Radar*, 2nd edition, IEE Radar, Sonar, And Navigation, Series 15, 2004.
4. Poljak, D. and V. Doric, "Wire antenna model for transient analysis of simple grounding systems, Part II: The horizontal grounding electrode," *Progress In Electromagnetics Research*, Vol. 64, 167–189, 2006.
5. Shoory, A., R. Moini, S. H. H. Sadeghi, and V. A. Rakov,

- “Analysis of lightning radiated electromagnetic fields in the vicinity of lossy ground,” *IEEE Trans. Electromagn. Compat.*, Vol. 47, No. 1, 131–145, 2005.
6. Sommerfeld, A., “Über die Ausbreitung der Wellen in der drahtlosen Telegraphie,” *Ann. Phys.*, Vol. 28, 665–736, 1909.
  7. Sommerfeld, A., *Partial Differential Equations*, 246–267, Academic Press, New York, 1949.
  8. Banos, A., *Dipole Radiation in the Presence of a Conducting Halfspace*, Pergamon Press, New York, 1966.
  9. Rahmat-Samii, Y., R. Mittra, and P. Parhami, “Evaluation of Sommerfeld integrals for lossy half-space problems,” *Electromagnetics*, Vol. 1, No. 1, 1–28, 1981.
  10. Burke, G. J., E. K. Miller, J. N. Brittingham, D. L. Lager, R. J. Lytle, and J. T. Okada, “Computer modeling of antennas near the ground,” *Electromagnetics*, Vol. 1, No. 1, 29–49, 1981.
  11. Mohsen, A., “On the evaluation of Sommerfeld integrals,” *IEE Proc. H, Microwaves, Opt. & Antennas*, Vol. 129, No. 4, 177–182, 1982.
  12. Michalski, K. A. and C. M. Butler, “Evaluation of Sommerfeld integrals arising in the ground stake antenna problem,” *IEE Proc.*, Vol. 134, No. 1, Pt. H, Feb. 1987.
  13. Siegel, M. and R. W. P. King, “Electromagnetic fields in a dissipative half-space, a numerical approach,” *J. Appl. Phys.*, Vol. 41, No. 6, 2415–2423, 1970.
  14. Tsang, L., R. Brown, J. A. Kong, and G. Simmons, “Numerical evaluation of electromagnetic fields due to dipole antennas in the presence of stratified media,” *Geophys. Res.*, Vol. 79, 2077–2080, 1974.
  15. Kuo, W. C. and K. K. Mei, “Numerical approximations of the Sommerfeld integral for fast convergence,” *Radio Sci.*, Vol. 13, No. 3, 407–415, 1978.
  16. Lin, C. C. and K. K. Mei, “Radiation and scattering from partially buried vertical wires,” *Electromagnetics*, Vol. 2, No. 4, 309–334, 1982.
  17. Katehi, P. B. and N. G. Alexopoulos, “Real axis integration of Sommerfeld integrals with applications to printed circuit antennas,” *J. Math. Phys.*, Vol. 24, No. 3, 527–533, 1983.
  18. Johnson, W. A. and D. G. Dudley, “Real axis integration of Sommerfeld integrals: Source and observation points in air,” *Radio Sci.*, Vol. 18, 175–186, 1983.
  19. Michalski, K. A., “On the efficient evaluation of integrals arising

- in the Sommerfeld half space problem," *IEE Proc. H, Microw., Antenna & Propag.*, Vol. 132, 312–318, 1985.
20. Miller, E. K., A. J. Poggio, G. J. Burke, and E. S. Selden, "Analysis of wire antennas in the presence of a conducting halfspace. Part I. The vertical antenna in free space," *Canadian J. Phys.*, Vol. 50, 879–888, 1972.
  21. Sarkar, T. K., "Analysis of arbitrarily oriented thin wire antennas over a plane imperfect ground," *Arch. Elek. Ubertragungstechn., Electronics and Communications*, Vol. 31, 449–457, 1977.
  22. Fuller, J. A. and J. R. Wait, "A pulsed dipole in the earth," *Transient Electromagnetic Fields*, L. B. Felsen (ed.), 237–269, Springer, 1976.
  23. Kong, J. A., L.-C. Shen, and L. Tsang, "Field of an antenna submerged in a dissipative dielectric medium," *IEEE Trans. Antennas Propag.*, Vol. 25, 887–889, 1977.
  24. Franssens, G. R., "Calculation of synthetic seismograms in layered media by means of a modified propagator matrix method," *Hybrid Formulation of Wave Propagation and Scattering*, L. B. Felsen (ed.), 357–373, Martinus Nijhoff, 1984.
  25. Yokoyama, A., "Dipole radiation affected by the plane earth," *Phys. Soc. Jpn.*, Vol. 27, 224–229, 1969.
  26. Chang, D. C. and J. R. Wait, "Appraisal of near-field solutions for a Hertzian dipole over a conducting half-space," *Canadian J. Phys.*, Vol. 48, 737–743, 1970.
  27. Kuo, W. C., "Numerical treatment of Sommerfeld's integrals and its application to antenna and scattering problems," Ph.D. Thesis, Electrical Engineering Department, University of California, Berkeley, 1973.
  28. Chang, D. C. and R. J. Fisher, "A unified theory on radiation of a vertical electric dipole above a dissipative earth," *Earth Sci.*, Vol. 9, 1129–1138, 1974.
  29. Linsay, Jr., J. E., "A direct approach to the numerical evaluation of electromagnetic fields due to sources buried beneath the earth's surface," *IEEE-AP International Symposium*, Boulder, Colorado, 1973.
  30. Wait, J. R., "Image theory of a quasistatic magnetic dipole over a dissipative half-space," *Electron. Lett.*, Vol. 5, No. 13, 281–282, 1969.
  31. Weaver, J. T., "Image theory for an arbitrary quasistatic field in the presence of a conducting half-space," *Radio Sci.*, Vol. 6, 647–653, 1971.

32. Bannister, P. R., "Summary of image theory expansions for the quasistatic fields of antennas at or above the earth's surface," *Proc. IEEE*, Vol. 67, 1001–1008, 1979.
33. Mittra, R., P. Parhami, and Y. Rahmat-Samii, "Solving the current element problem over lossy half-space without Sommerfeld's integrals," *IEEE Trans. Antennas Propag.*, Vol. 27, 778–782, 1979.
34. Mahmoud, S. F., "Image theory for electric dipoles above a conducting anisotropic earth," *IEEE Trans. Antenna Propag.*, Vol. 32, 679–683, 1984.
35. Lindell, I. and E. Alanen, "Exact image theory for the Sommerfeld half-space problem — Part I: Vertical magnetic dipole," *IEEE Trans. Antennas Propag.*, Vol. 32, 126–133, 1984.
36. Lindell, I. and E. Alanen, "Exact image theory for the Sommerfeld half-space problem — Part II: Vertical electric dipole," *IEEE Trans. Antennas Propag.*, Vol. 32, 841–847, 1984.
37. Lindell, I. and E. Alanen, "Exact image theory for the Sommerfeld half-space problem — Part III: General formulation," *IEEE Trans. Antennas Propag.*, Vol. 32, 1027–1032, 1984.
38. Lindell, I., E. Alanen, and H. Von Bagh, "Exact image theory for the calculation of fields transmitted through a planar interface of two media," *IEEE Trans. Antennas Propag.*, Vol. 34, No. 2, 129–137, 1986.
39. Xu, X.-B. and Y. Huang, "An efficient analysis of vertical dipole antennas above a lossy half-space," *Progress In Electromagnetics Research*, Vol. 74, 353–377, 2007.
40. Collin, R. E., *Field Theory of Guided Waves*, McGraw-Hill, New York, 1960.
41. Kong, J. A., *Electromagnetic Wave Theory*, Wiley, New York, 1981.
42. Chew, W. C., *Waves and Fields in Inhomogeneous Media*, Van Nostrand, New York, 1990.
43. Felsen, L. B. and N. Marcuvitz, *Radiation and Scattering of Waves*, Prentice-Hall, 1973.
44. Brekhovskikh, L. M., *Waves in Layered Media*, Academic Press, 1980.
45. Parhami, P., Y. Rahmat-Samii, and R. Mittra, "An efficient approach for evaluating Sommerfeld integrals encountered in the problem of a current element radiating over lossy ground," *IEEE Trans. Antennas Propag.*, Vol. 28, 100–104, 1980.
46. Ling, R. T., J. D. Scholler, and P. Ya. Ufimtsev, "The propagation

- and excitation of surface waves in an absorbing layer,” *Progress In Electromagnetics Research*, Vol. 19, 49–91, 1998.
47. Tsang, L. and J. A. Kong, “Electromagnetic fields due to a horizontal electric dipole antenna laid on the surface of a two-layer medium,” *IEEE Trans. Antennas Propag.*, Vol. 22, 709–711, 1974.
  48. Dos Santos, A. F., “Electromagnetic-wave propagation along a horizontal wire above ground,” *Proc. IEE*, Vol. 119, 1103–1109, 1972.
  49. Tsang, L., C.-J. Ong, and B. Wu, “Electromagnetic fields of Hertzian dipoles in thin-layered media,” *IEEE Antennas Wireless Propag. Lett.*, Vol. 5, 537–540, Dec. 2006.
  50. Mosig, J. R. and T. K. Sarkar, “Comparison of quasistatic and exact electromagnetic fields from a horizontal electric dipole above a lossy dielectric backed by an imperfect ground plane,” *IEEE Trans. Microw. Theory Tech.*, Vol. 34, 379–387, Apr. 1986.
  51. Michalski, K. A., “Extrapolation methods for Sommerfeld integral tails,” *IEEE Trans. Antennas Propag.*, Vol. 46, No. 10, 1405–1418, Oct. 1998.
  52. Mosig, J. R. and F. E. Gardiol, “Analytical and numerical techniques in the Green’s functions treatment of microstrip antennas and scatterers,” *Proc. Inst. Elect. Eng. Microwave Antennas and Propagation*, Vol. 130, 175–182, Mar. 1983.
  53. Mosig, J. R. and A. A. Melcón, “Green’s functions in lossy layered media: Integration along the imaginary axis and asymptotic behavior,” *IEEE Trans. Antenna Propag.*, Vol. 51, 3200–3208, Dec. 2003.
  54. Demuynck, F. J., G. A. E. Vandenbosch, and A. R. Van de Capelle, “The expansion wave concept — Part I: Efficient calculation of the spatial Green’s functions in a stratified dielectric medium,” *IEEE Trans. Antenna Propag.*, Vol. 46, 397–406, 1998.
  55. Simsek, E., Q. H. Liu, and B. Wei, “Singularity subtraction for evaluation of Green’s functions for multilayer media,” *IEEE Trans. Microw. Theory Tech.*, Vol. 54, 216–225, Jan. 2006.
  56. Chow, Y. L., J. J. Yang, D. G. Fang, and G. E. Howard, “A closed-form spatial Green’s function for the thick microstrip substrate,” *IEEE Trans. Microw. Theory Tech.*, Vol. 39, No. 3, 588–592, Mar. 1991.
  57. Yang, J. J., Y. L. Chow, and D. G. Fang, “Discrete complex images of a three-dimensional dipole above and within a lossy ground,” *IEE Proc.*, Vol. 138, No. 4, Pt. H, 319–326, Aug. 1991.

58. Tang, J. L. and W. Hong, "The electromagnetic field produced by a horizontal electric dipole over a dielectric coated perfect conductor," *Progress In Electromagnetics Research*, Vol. 36, 139–152, 2005.
59. Zhang, H.-Q., W.-Y. Pan, K. Li, and K.-X. Shen, "Electromagnetic field for a horizontal electric dipole buried inside a dielectric layer coated high lossy half space," *Progress In Electromagnetics Research*, Vol. 50, 163–186, 2005.
60. Mei, J. P. and K. Li, "Electromagnetic field from a horizontal electric dipole on the surface of a high lossy medium coated with a uniaxial layer," *Progress In Electromagnetics Research*, Vol. 73, 71–91, 2007.
61. King, R. W. P., "On the radiation efficiency and the electromagnetic field of a vertical electric dipole in the air above a dielectric or conducting half-space," *Progress In Electromagnetics Research*, Vol. 4, 1–43, 1991.
62. Abramowitz, M. and I. Stegun, *Handbook of Mathematical Functions*, Dover, New York, 488, 1970.
63. Burke, G. J. and A. J. Poggio, *Numerical Electromagnetic Code (NEC)-method of Moments*, Vol. 116, Naval Ocean Syst. Control, San Diego, CA, 1980.
64. Burke, G. J., *Numerical Electromagnetic Code (NEC4)-method of Moments, Part 2: Program Description-theory*, Lawrence Livermore National Laboratory, UCRL-MA-109338, 1992.